Original
ISSN 2413-0516

Docking Study, Synthesis, Characterization and Preliminary Cytotoxic Evaluation of New 1,3,4-Thiadiazole Derivatives

Noor M. Mohammed[1,3*], Mohammed Hassan Mohammed[1], Zainab M. Abdulkhaleq[2]

[1]Department of Pharmaceutical Chemistry, College of Pharmacy, University of Baghdad, Baghdad, Iraq.
[2]Department of Pharmacy, Al-Mustafa University College, Baghdad, Iraq.
[3]Department of Pharmacy, Al-Farabi University College, Baghdad, Iraq.
*Correspondence to: Noor M. Mohammed (E-mail: non.myo.86@gmail.com)
(Submitted: 03 May 2023 – Revised version received: 29 May 2023 – Accepted: 18 June 2023 – Published Online: 26 August 2023)

Abstract

Objectives: This study has determined that these newly synthesized analogs hold promise as potential sources of novel anticancer agents for combating breast cancer.

Methods: We initiated our research by obtaining the crystal structure of Histone deacetylases (HDACs-8) bound with Vorinostat (SAHA) from the Protein Data Bank (PDB code 4QA0). Subsequently, we conducted docking experiments, which revealed that compounds (V c,s, V d,s, V c,t, and V d,t) exhibited favorable docking scores when compared to the standard. These compounds, synthesized through multi-step procedures involving the reaction of intermediate derivatives (IV c,d) with thiosemicarbazide or semicarbazide, were subjected to confirmation of their chemical structures using FT-IR and ^{1}H NMR analysis.

Results: The results of our *in-vitro* cytotoxicity assay (MTT assay) highlighted that compounds V c,t and V d,t exhibited notable inhibition ratios in the breast cancer cell line (MCF-7), while V c,t displayed similar efficacy in human colon adenocarcinoma (HRT-18) compared to the control drug, Vorinostat (SAHA).

Conclusion: Our docking analysis led us to conclude that the C=S moiety demonstrated exceptional binding affinity to the zinc binding group of the HDAC enzyme, establishing multiple interaction modes. This finding suggests the potential of these compounds as valuable candidates in the development of anticancer treatments.

Keywords: Anticancer, thiadiazoles, MCF-7, HRT-18, docking study

Introduction

Epigenetic changes in cancer are common and associated with pathogenesis and molecular heterogeneity.[1] Carcinogenesis results from the interplay between the activation of oncogenes and the inactivation of tumor suppressor genes. One of the causes of the latter is switching off the gene in concern by epigenetic changes rather than by mutation of the DNA sequence. These reversible epigenetic changes do not involve alteration of the nucleotide sequence of DNA but, instead, are due to inappropriate DNA methylation, chromatin remodeling, and changes in small noncoding RNAs.[2]

Epigenetic mechanisms that modify chromatin structure can be divided into four main categories: DNA methylation, covalent histone modifications, non-covalent mechanisms such as incorporating histone variants, and nucleosome remodeling and non-coding RNAs, including miRNAs.[3] These modifications work together to regulate the functioning of the genome by altering the local structural dynamics of chromatin, primarily controlling its accessibility and compactness. The interplay of these modifications creates an 'epigenetic landscape' that regulates the way the mammalian genome manifests itself in different cell types, developmental stages, and disease states, including cancer.[4]

Histone deacetylases (HDACs) have received significant attention in the research area of epigenetics. Acetylation by HATs transfers an acetyl group and neutralizes the positive charge of lysine residues in the histone tail resulting in loosening histone–DNA interactions and allowing access of transcription factors to DNA. The stimulatory effect of HATs on gene expression is reversed by HDACs, which remove an acetyl group from the terminal amino group of a lysine residue, leaving a positive charge, that tightly interacts with the negative amount of DN, promotes chromatin condensation, and thereby repress transcription and induce gene silencing. Thereby, HATs are co-activators, and the HDACs are co-repressors.[5]

Any imbalance between the activities of these two opposite enzyme families would disturb the normal histone acetylation homeostasis. Overexpression of HDACs, i.e., hypoacetylation, is involved in cancer generation and cancer progress since tumor suppressor gene transcription is prevented due to the inactivated chromatin system. There would be alteration in proliferation, differentiation, and apoptosis fashion of normal cells becoming malignant. Hypoacetylation is also involved in the loss of cell adhesion, migration, invasion, and angiogenesis, resulting in cancer start and progress.[6]

HDACs are overexpressed in several types of cancer cells compared to normal cells. For example, breast cancer cells show measurable levels of HDACs 1, 2, and 3, while normal breast cells do not show any.[7,8] This finding could be of great clinical value for targeting these enzymes in breast cancer. Besides, the specificity of HDACIs against the other types of cancer cells is still of great importance; the importance of inhibition of elevated levels of these enzymes in cancer cells outweighs inhibition of low levels in normal cells. Furthermore, the relative specificity of HDACIs between cancer cells and normal cells may be attributed to the idea hypothesized that, in contrast to cancer cells, normal cells could withstand the inhibitory action of HDACIs and compensate for the inhibited vital pathways since they have multiple, alternative epigenetic regulatory ways.[9]

Histone deacetylase inhibitors (HDACIs) have emerged as a new class of anti-cancer agents that play essential roles in

epigenetic regulation of gene expression, inducing death, apoptosis, and cell cycle arrest in cancer cells. Several HDACIs with much more potent anticancer effects and diverse structures have been identified; they include natural or synthetic products.[10] Recently, many HDAC inhibitors have been clinically validated in cancer patients resulting in the approval of five HDACIs, vorinostat, romidepsin, belinostat and panobinostat by the FDA and chidamide by Chinese FDA for the treatment of cutaneous, peripheral T-cell lymphoma (CTCL, PTCL) multiple myeloma (MM) and acute myeliod leukemia (AML).[11,12] SAHA, belinostat, and panobinostat are pan-HDACIs since they targeting multiple HDAC isoforms, while romidepsin is a selective one.[13,14] Several new HDACIs are in different stages of clinical development for the treatment of hematological malignancies as well as solid tumors. HDACIs have the potential to be used as monotherapies or in combination with other anticancer therapies.[15] Also, great efforts are exerted to discover novel HDACIs for use as anticancer drugs alone or in combination and have isoform selectivity are continuing by researchers.[16]

The "classical" HDAC-Is act exclusively on HDAC Classes I, II and IV by binding to the zinc-enriched catalytic domain of the HDACs. Figure 1 show the main four classes of HDAC inhibitors and the FDA-approved ones. Classical HDAC-Is are subdivided according to the chemical moiety that binds to the zinc ion (except cyclic tetrapeptides which bind to the zinc ion with a thiol group). Some examples in decreasing order of the typical zinc binding affinity:[17]

1. Hydroxamic acids (or hydroxamates) the major group, such as Vorinostat (SAHA), Belinostat and Panobinostat,
2. Cyclic tetrapeptides such as Romidepsin or Depsipeptides,
3. Benzamides or o-aminoanilides, Mocetinostat, Chidamide and Entinostat,
4. The aliphatic acid such as Phenylbutyrate and Valproic acid.

The 1,3,4-thiadiazole is a unique five membered ring system, Figure 2 that has acquired noticeable quality by exploring wide spectrum of biological activity, due to the existence of the -N=C–S component.[18] Many compounds with 1,3,4- thiadiazole moiety have a wide range of therapeutic effects, such as anti-bacterials,[19] anti-fungals,[20] anti-mycobacterials,[21] analgesics, anti-inflammatory,[22] anti- psychotics[23] and anti-convulsants.[24] Compounds with 1,3,4-thiadiazole moiety exhibited remarkable anti-cancer activity.[25-30]

Materials and Methods

Materials

4-nitrobenzyldehyde, 4-methoxybenzaldehyde was purchased from HyperChem China. Other chemicals were purchased from Sigma–Aldrich. All chemicals are of analytical grade, and they were used as received without further purification.

Characterization of Compounds (V c,s, V d,s, Vc,t and V d,t)

Melting points, Fourier transform infrared spectroscopy: FTIR, NMR: ^{1}H-NMR spectra, were performed for compound characterization.

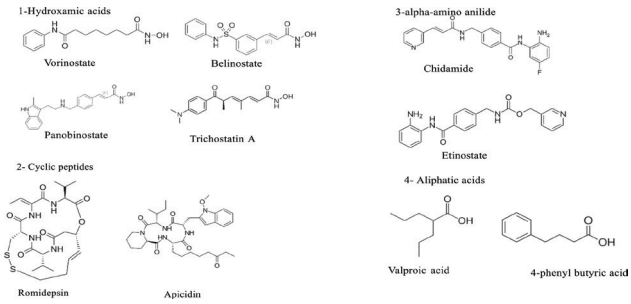

Fig. 1 **The main four classes of HDAC inhibitors.**

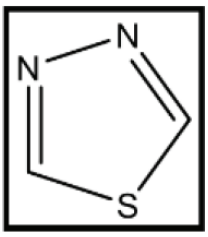

Fig. 2 **Chemical structure of 1,3,4-Thiadiazole.**

Molecular Docking

Vorinostat (SAHA) was used to validate the docking process because the PDB obtained has a crystal structure of the protein and bound Vorinostat (SAHA).

Histone Deacetylase Enzyme[31,32]

The Molecular Operating Environment (MOE) software version 2015.10 was used to conduct the docking studies (Chemical Computing Group, Montreal, Canada). HDAC-8 (PDB code 4QA0) X-ray crystal structures were retrieved from the Protein Data Base (PDB).

All water molecules were removed from PDB files, and hydrogen atoms were then added to the protein. The MOE-Dock algorithm was then used to dock the optimized shape of the chemical into the binding site.

The London dG was selected as the initial scoring method and the Rigid Receptor was selected as the final scoring method. The best 5 poses of each ligand were retained and scored. Finally, the geometry of docked complex was analyzed by the pose viewer utility in MOE.

Chemical Synthesis

The target compounds were synthesized by multi-step reactions, as shown in Scheme 1.

Synthesis of Dihydropyrimidine derivatives (I c,d)

A mixture of aldehydes (10 mmol), Ethyl acetoacetate (10 mmol), urea (15 mmol) and 10 ml of ethanol and (4 mmol) of Ammonium chloride, was refluxed for 7–8 hours. Then the reaction mixture was neutralized with 1N HCl. The precipitate was filtered and recrystallized from ethanol.[33]

The title ethyl 6-methyl-4-(4-nitrophenyl)-2-oxo-1,2,3,4-tetrahydropyrimidine-5-carboxylate (I c) was obtained as a pale-yellow powder, mp. 203-206°C, yield 91%. The FT-IR for I c, 3232 cm^{-1} N-H str. Vibration of amide, 2985 cm^{-1} C-H Asymmetric str. Vibration of aliphatic CH_2, 1701 cm^{-1} Carbonyl str. vibration band of ester, 1643 cm^{-1} Carbonyl str. vibration band of amide, 1303 cm^{-1} C-N str. Vibration of

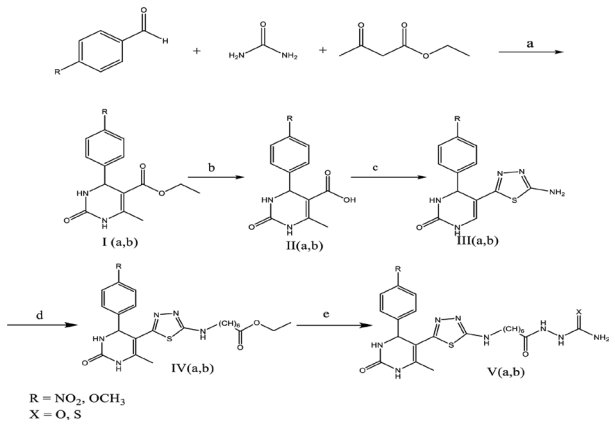

Scheme 1. **Synthesis schematics of compound (V c,s – V d,t). Reagents and conditions: (a) Reflux 7–8 hr. abs. ethanol (b) Hydrolysis by 15% NaOH(c) Thiosemicarbazide, 70% sulfuric acid in ethanol, ammonia (d) Ethyl-7-bromoheptanoate, dry K_2CO_3 in anhydrous acetone (e) Thiosemicarbazide, semicarbazide, methanol, KOH.**

amide, 1211 cm^{-1} C-O str. Vibration of ester. 1H NMR (400 MHz, DMSO-d6) δ 1.123-1.152(t, J = 5.0 Hz, 3H), 4.159-4.202(q, J = 4.1 Hz, 2H), 2.3141(s, J = 7.2 Hz, 3H), 5.415-5.428(d, J = 5.0 Hz, 1H), 7.527-7.542(d, 3H), 8.167-8.184(d, 2H), 9.901(s, 1H). And ethyl 4-(4-methoxyphenyl)-6-methyl-2-oxo-1,2,3,4-tetrahydropyrimidine-5-carboxylate compound (I d) was obtained as a yellow powder mp. 201-203°C, yield 81%. The FT-IR for I d, 3240 cm^{-1} N-H str. Vibration of amide, 2981 cm^{-1} C-H Asymmetric str. Vibration of aliphatic CH_2, 1701 cm^{-1} Carbonyl str. vibration band of ester, 1647 cm^{-1} Carbonyl str. vibration band of amide, 1307 cm^{-1} C-N str. Vibration of amide, 1219 cm^{-1} C-O str. Vibration of ester. ^{1}H NMR (400 MHz, DMSO-d6) δ 1.123-1.152(t, J = 5.0 Hz, 3H), 4.159-4.202(q, J = 4.1 Hz, 2H), 2.3141(s, J = 7.2 Hz, 3H), 5.110-5.125(d, J = 5.0 Hz, 1H), 6.880-6.897(d, 2H), 7.292-7.306(d, 2H), 7.527-7.542(d, 1H), 9.901(s, 1H).

Ester Hydrolysis (II c,d)

A stirring mixture of compounds (I c,d) (10 mmol) and sodium hydroxide (15%, 10 ml) was refluxed for 12–15 hours at 90°C. After cooling, the solution was acidified with (1N) hydrochloric acid and the precipitate was filtered and recrystallized from ethanol.[34]

The title 6-methyl-4-(4-nitrophenyl)-2-oxo-1,2,3,4-tetrahydropyrimidine-5-carboxylic acid (II c) was obtained as a white powder, mp. 219-221°C, yield 80%. The FT-IR for II c, 3400-2800 cm^{-1} O-H Vibration of carboxylic acid, 3100 cm^{-1} C-H Asymmetric str. Vibration of an aromatic ring, 1701 cm^{-1} Carbonyl str. vibration band of carboxylic acid. 1662 cm^{-1} Carbonyl str. vibration band of amide, 1284 cm^{-1} C-N str. Vibration of amide. ^{1}H NMR (400 MHz, DMSO-d6) δ 12.36 (s, 1H), 9.90 (s, 1H), 8.18 (d, J = 8.6 Hz, 2H), 7.58 (d, J = 8.1 Hz, 2H), 7.32 (d, J = 7.3 Hz, 1H), 5.34 (d, J = 8.9 Hz, 1H), 2.23 (s, 3H). And 4-(4-methoxyphenyl)-6-methyl-2-oxo-1,2,3,4-tetrahydropyrimidine-5 carboxylic acid compound (II d) was obtained as a white powder mp. 218-219°C, yield 75%. The FT-IR for II d, 3400-2800 cm^{-1} O-H Vibration of carboxylic acid, 3012 cm^{-1} C-H Asymmetric str. Vibration of an aromatic ring, 1687 cm^{-1} Carbonyl str. vibration band of carboxylic acid, 1597 cm^{-1} Carbonyl str. vibration band of amide, 1315 cm^{-1} C-N str. Vibration of amide, 1022 cm^{-1} str. Vibration of ether. ^{1}H NMR (400 MHz, DMSO-d6) δ 12.36 (s, 1H), 9.90 (s, 1H), 7.32 (d, J = 7.3 Hz, 1H), 7.23 (d, J = 8.5 Hz, 2H), 6.89 (d, J = 8.3 Hz, 2H), 5.33 (d, J = 7.3 Hz, 1H), 3.78 (s, 3H), 2.23 (s, 3H).

Synthesis of 1,3,4- Thiadizole-2-amino derivatives synthesis (III c,d)

A mixture of thiosemicarbazide (5 mmol), compounds (II c,d) (5 mmol) and 70% sulfuric acid in ethanol. Was cool and stirred overnight and then refluxed at a temperature of 80–90°C for 7 hours. The reaction mixture was cool and neutralized with concentrated ammonia checked by litmus paper to PH 4. The precipitate was filtered and recrystallized from ethanol.[35]

The title 5-(5-amino-1,3,4-thiadiazol-2-yl)-4-(4-nitrophenyl)-6-methyl-3,4-dihydropyrimidin-2(1H)-one compound (III c) was obtained as off-white powder, mp. 168–170°C, yield 74%. The FT-IR for III c, 3421 cm^{-1} N-H str. Vibration of amide, 3352-3286 cm^{-1} N-H str. Vibration of primary amine, 3035 cm^{-1}C-H Asymmetric str. Vibration of aromatic ring, 1577 cm^{-1}C=C str. Vibration of aromatic ring, 1303 cm^{-1} C-N str. Vibration of amide, 725 cm^{-1} C-S-C str. vibration band. ^{1}H NMR (400 MHz, DMSO-d6) δ 10.02 (s, 1H), 8.19 – 8.14 (m, 3H), 7.54 (d, J = 8.9 Hz, 2H), 7.02 (s, 2H), 5.75 (d, J = 7.4 Hz, 1H), 2.19 (s, 3H). The title 5-(5-amino-1,3,4-thiadiazol-2-yl)-4-(4-methoxyphenyl)-6-methyl-3,4-dihydropyrimidin-2(1H)-one compound (III d) was obtained as off-white powder, mp. 166–168°C, yield 75%. The FT-IR for III d, 3352 cm^{-1} N-H str. Vibration of amide, 3012 cm^{-1} C-H Asymmetric str. Vibration of aromatic ring, 1620 cm^{-1} carbonyl str. Vibration of amide, 1300 cm^{-1} C-N str. Vibration of amide, 1017 cm^{-1} C-O-C str. Vibration of ether, 712 cm^{-1} C-S-C str. vibration band. ^{1}H NMR (400 MHz, DMSO-d6) δ 10.02 (s, 1H), 8.14 (d, J = 7.3 Hz, 1H), 7.29 (d, J = 8.5 Hz, 2H), 7.02 (s, 2H), 6.90 (d, J = 8.2 Hz, 2H), 5.69 (d, J = 7.4 Hz, 1H), 3.78 (s, 3H), 2.19 (s, 3H).

Amine Alkylation (IV c,d)

A mixture of compound (III c,d) (7.9 mmol), ethyl-7-bromoheptanoate (7.9 mmol) and dry K_2CO_3 (23.8 mmol) in anhydrous acetone (20 mL) was stirred under reflux. After 24 hours at 70°C. Upon completion of the reaction (as indicated by TLC), the solvent was reduced. The resulted precipitate was filtered and washed with distilled water and recrystallized from ethanol.[36]

The title ethyl ethyl 7-((5-(6-methyl-4-(4-nitrophenyl)-2-oxo-1,2,3,4-tetrahydropyrimidin-5-yl)-1,3,4-thiadiazol-2-yl) amino) heptanoate compound (IV c) was obtained as a white powder mp. 198–200°C, yield 83%. The FT-IR for IV c, 3383 cm^{-1} N-H str. Vibration of amide, 3066 cm^{-1} C-H Asymmetric str. Vibration of an aromatic ring, 1732 cm^{-1} Carbonyl str. vibration band of ester, 1705 cm^{-1} Carbonyl str. vibration band of amide, 1604 cm^{-1} C=N str. Vibration, 1573 cm^{-1} C=C Symmetric str. Vibration of aromatic ring, 1462 cm^{-1} C-H asymmetric and symmetric str. Vibration of $(CH_2)_6$, 1377 cm^{-1} C-H asymmetric and symmetric str. Vibration of $(CH_2$-$CH_3)$, 1315 cm^{-1} C-N str. Vibration of amide, 1199 cm^{-1} O-C str. Vibration, 698 cm^{-1} C-S-C str. Vibration. ^{1}H NMR (400 MHz, DMSO-d6) δ 9.97 (s, 1H), 8.20 – 8.14 (m, 3H), 7.54 (d, J = 8.0 Hz, 2H), 7.50 (t, J = 4.7 Hz, 1H), 5.75 (d, J = 8.0 Hz, 1H), 4.10 (q, J = 6.6 Hz, 2H), 3.46 (q, 2H), 2.29 (t, J = 8.5 Hz, 2H), 2.19 (s, 3H), 1.67 – 1.49 (m, 4H), 1.40 – 1.24 (m, 4H),

1.16 (t, J = 6.6 Hz, 3H). And ethyl 7-((5-(4-(4-methoxyphenyl)-6-methyl-2-oxo-1,2,3,4-tetrahydropyrimidin-5-yl)-1,3,4-thiadiazol-2-yl) amino) heptanoate compound (IV d) was obtained as pale-yellow powder mp. 196–198°C, yield 90%. The FT-IR for IV d, 3278 cm^{-1} N-H str. Vibration of amide, 2935 cm^{-1} C-H Asymmetric str. Vibration of aliphatic CH_3, 1732 cm^{-1} Carbonyl str. vibration band of ester, 1681 cm^{-1} Carbonyl str. vibration band of amide, 1597 cm^{-1}C=N str. Vibration, 1462 cm^{-1} C=C Symmetric str. Vibration of aromatic ring, 1427 cm^{-1} C-H asymmetric and symmetric str. Vibration of $(CH_2)_6$, 1373 cm^{-1} C-H asymmetric and symmetric str. Vibration of (CH_2- CH3), 1315 cm^{-1} C-N str. Vibration of amide, 1157 cm^{-1} O-C str. Vibration, 1026 cm^{-1} C-O-C str. Vibration of ether, 698 cm^{-1} C-S-C str. Vibration. ^{1}H NMR (400 MHz, DMSO-d6) δ 9.97 (s, 1H), 8.14 (d, J = 7.4 Hz, 1H), 7.50 (t, J = 4.7 Hz, 1H), 7.29 (d, J = 8.1 Hz, 2H), 6.90 (d, J = 8.2 Hz, 2H), 5.69 (d, 1H), 4.10 (q, J = 6.6 Hz, 2H), 3.78 (s, 3H), 3.46 (q, 2H), 2.29 (t, J = 8.5 Hz, 2H), 2.19 (s, 3H), 1.67 – 1.49 (m, 4H), 1.40 – 1.24 (m, 4H), 1.16 (t, J = 6.6 Hz, 3H).

Synthesis of Amid (V c,s – V d,t)

To a solution of thiosemicarbazide or semicarbazide (34.8 mmol) in 10 mL methanol, KOH (34.8 mmol) was added. The reaction mixture was stirred for 10 min at 40°C, and was then cooled to 0°C and filtered. Compound (IV c,d) (320 mg, 1.1 mmol) was added to the filtrate, after which the reaction was stirred at room temperature for 30 min. The solvent was removed under reduced pressure, diluted with a saturated Ammonium chloride aqueous solution, and extracted with ethyl acetate. The organic layer was dried over Sodium sulfate. The resulting solution was evaporated under reduced pressure.[37]

The title 2-(7-((5-(6-methyl-4-(4-nitrophenyl)-2-oxo-1,2,3,4-tetrahydropyrimidin-5-yl)-1,3,4-thiadiazol-2-yl) amino) heptanoyl) hydrazine-1-carboxamide Compound (V c,s) was obtained as off-white powder mp. 265-267°C, yield 80%. The FT-IR for V c,s, 3468 cm^{-1} N-H str. Vibration of secondary amide, 3309,3267 cm^{-1} N-H str. Vibration of primary amide 2985 cm^{-1} C-H Asymmetric str. Vibration of aliphatic CH_3, 1681 cm^{-1} Carbonyl str. vibration band of dihydropyrimidin ring, 1647 cm^{-1} Carbonyl str. vibration band of amide $(CH_2)_6$, 1604 cm^{-1} Carbonyl str. vibration band of primary amide, 1573 cm^{-1} C=N str. Vibration, 1531 cm^{-1} C=C Symmetric str. Vibration of aromatic ring, 1462 cm^{-1} C-H asymmetric and symmetric str. Vibration of $(CH_2)_6$, 1288cm^{-1} C-N str. Vibration of amide, 698 cm^{-1} C-S-C str. Vibration. ^{1}H NMR (400 MHz, DMSO-d6) δ 9.97 (s, 1H), 9.62 (d, J = 6.4 Hz, 1H), 8.95 (d, J = 6.4 Hz, 1H), 8.20 – 8.14 (m, 3H), 7.54 (d, J = 8.5 Hz, 2H), 7.50 (t, J = 4.6 Hz, 1H), 6.44 (s, 2H), 5.75 (d, J = 7.5 Hz, 1H), 3.46 (q, 2H), 2.24 – 2.17 (m, 5H), 1.67 – 1.51 (m, 4H), 1.40 – 1.28 (m, 4H). The title 2-(7-((5-(4-(4-methoxyphenyl)-6-methyl-2-oxo-1,2,3,4-tetrahydropyrimidin-5-yl)-1,3,4-thiadiazol-2-yl) amino) heptanoyl) hydrazine-1-carboxamide compound (V d,s) was obtained as a pale yellow powder mp. 170-172°C, yield 85%. The FT-IR for V d,s, 3452 cm^{-1} N-H str. Vibration of secondary amide, 3271,3197 cm^{-1} N-H str. Vibration of primary amide 2954 cm^{-1} C-H Asymmetric str. Vibration of aliphatic CH_3, 1681 cm^{-1} Carbonyl str. vibration band of dihydropyrimidin ring, 1647 cm^{-1} Carbonyl str. vibration band of amide $(CH_2)_6$, 1597 cm^{-1} Carbonyl str. vibration band of primary amide, 1573 cm^{-1} C=N str. Vibration, 1508 cm^{-1} C=C Symmetric str. Vibration of aromatic ring, 1427 cm^{-1} C-H asymmetric and symmetric str. Vibration of $(CH_2)_6$, 1303cm^{-1} C-N str. Vibration of amide, 1026 cm^{-1} C-O-C str. Vibration of ether, 698 cm^{-1}C-S-C str. Vibration. The ^{1}H NMR (500 MHz, DMSO-d6) δ 9.97 (s, 1H), 9.62 (d, J = 6.4 Hz, 1H), 8.95 (d, J = 6.4 Hz, 1H), 8.14 (d, J = 7.3 Hz, 1H), 7.50 (t, J = 4.6 Hz, 1H), 7.29 (d, J = 8.2 Hz, 2H), 6.90 (d, J = 8.3 Hz, 2H), 6.44 (s, 2H), 5.69 (d, J = 7.1 Hz, 1H), 3.78 (s, 3H), 3.47 (q, 2H), 2.24 – 2.17 (m, 5H), 1.67 – 1.51 (m, 4H), 1.40 – 1.28 (m, 4H). The title 2-(7-((5-(6-methyl-4-(4-nitrophenyl)-2-oxo-1,2,3,4-tetrahydropyrimidin-5-yl)-1,3,4-thiadiazol-2-yl) amino) heptanoyl) hydrazine-1-carbothioamide compound (V c,t) was obtained as a pale yellow powder mp. 200-202°C, yield 79%. The FT-IR for V c,t, 3162 cm^{-1} N-H str. Vibration of secondary amide, 3135, 2981 cm^{-1} N-H str. Vibration of primary amide 2896 cm^{-1} C-H Asymmetric str. Vibration of aliphatic CH_3, 1701 cm^{-1} Carbonyl str. vibration band of dihydropyrimidin ring, 1643 cm^{-1} Carbonyl str. vibration band of amide $(CH_2)_6$, 1604 cm^{-1} C=N str. Vibration, 1577 cm^{-1} C=C Symmetric str. Vibration of aromatic ring, 1465 cm^{-1} C-H asymmetric and symmetric str. Vibration of $(CH_2)_6$, 1288 cm^{-1} C-N str. Vibration of amide, 1261 cm^{-1} C=S str. Vibration, 682 cm^{-1} C-S-C str. Vibration. ^{1}H NMR (400 MHz, DMSO-d6) δ 10.05 (d, J = 5.4 Hz, 1H), 9.97 (s, 1H), 9.08 (d, J = 5.1 Hz, 1H), 8.20 – 8.14 (m, 3H), 7.54 (d, J = 8.5 Hz, 2H), 7.50 (t, J = 4.6 Hz, 1H), 7.28 (s, 2H), 5.75 (d, J = 7.6 Hz, 1H), 3.47 (q, 2H), 2.24 – 2.17 (m, 5H), 1.67 – 1.51 (m, 4H), 1.40 – 1.28 (m, 4H). The title 2-(7-((5-(4-(4-methoxyphenyl)-6-methyl-2-oxo-1,2,3,4-tetrahydropyrimidin-5-yl)-1,3,4-thiadiazol-2-yl) amino) heptanoyl) hydrazine-1-carbothioamide compound (V d,t) was obtained as a pale off-white powder mp. 199-201°C, yield 82%. The FT-IR for V d,t, 34331 cm^{-1} N-H str. Vibration of secondary amide, 3167 cm^{-1} N-H str. Vibration of primary amide 2970 cm^{-1} C-H Asymmetric str. Vibration of aliphatic CH_3, 1678 cm^{-1} Carbonyl str. vibration band of amide $(CH_2)_6$, 1573 cm^{-1} C=N str. Vibration, 1593 cm^{-1} C=C Symmetric str. Vibration of aromatic ring, 1427 cm^{-1} C-H asymmetric and symmetric str. Vibration of $(CH_2)_6$, 1315cm^{-1} C-N str. Vibration of amide, 1253 cm^{-1} C=S str. Vibration, 1022 cm^{-1} C-O-Cl str. Vibration of ether, 686 cm^{-1} C-S-C str. Vibration. ^{1}H NMR (400 MHz, DMSO-d6) δ 10.05 (d, J = 5.4 Hz, 1H), 9.97 (s, 1H), 9.08 (d, J = 5.1 Hz, 1H), 8.14 (d, J = 7.3 Hz, 1H), 7.50 (t, J = 4.6 Hz, 1H), 7.28 (d, 3H), 6.90 (d, J = 8.3 Hz, 2H), 5.69 (d, J = 7.1 Hz, 1H), 3.78 (s, 3H), 3.47 (q, 2H), 2.24 – 2.17 (m, 5H), 1.67 – 1.51 (m, 4H), 1.40 – 1.28 (m, 4H).

In Vitro Cytotoxicity Assay[38,39]

The *in vitro* cytotoxicity of compounds V c,s, V d,s, V c,t, and V dd,t were evaluated by MTT assay on human breast cancer cells (MCF-7) and human colon adenocarcinoma (HRT-18). MTT was performed to determine the cytotoxic effect of the samples at various concentrations. The results were given as the mean of three independent experiments and the IC_{50} values were then calculated.

Statistical Analysis

The results of the experimental work were demonstrated as the standard error of the mean (SEM) for triplicate data by using nonlinear regression analysis (Prism Pad 8.1).

Results

Molecular Docking

Binding Site of SAHA

The binding site of HDAC-8 is formed like a cleft which contains a deep pocket that mainly made up of Phe152, Met274, Gly152, His142, His143, Trp142, Gly304, Tyr306, Asp187, Asp267, Asp101, His180 and Phe208. The deep pocket prefers non hydrophobic moieties such as NH and C=S fragments.

According to the result of docking as shown in Table 1 and Figures 3-7, V c,s, V d,s, V c,t, and V d,t give very good docking scores compared to the standard (SAHA) since synthetic compounds interacted with the most residues in the active site (predominantly hydrogen bond).

The V c,t appear to has more binding tendency with HDAC-8 via zinc binding group(C=S) spacer and also thiadiazol ring (good fitting) (His142, His143 and Zn401) while V c,s which bind through zinc binding group (C=O), The C=S group of the V c,t aid to more binding tendency (good fitting) (Tyr306 and Zn401) due to the effect of zinc binding group than C=O of V d,s.

Table 1. **The results of interactions of the ligands with HDAC-8**

Compound ID	Docking score (kcal/mol)	H-bond interaction	Coordinating bond length (with zinc) [Å]
SAHA	–8.69	Tyr306(2.98)	2.17
V c,s	–9.50	Asp178(3.28), Asp101(3.54), Tyr306(3.19), His143(3.13), Lys33(3.24), Lys33(3.40)	1.96
V d,s	–9.91	Asp178(3.03), Gly206(3.80), His143(3.14)	1.99
V c,t	–8.17	Gly151(2.79), Asp101(3.42), His142(3.66), Hiis143(3.37)	2.15
V d,t	–8.21	Gly151(2.80), Tyr306(3.19), His143(3.09)	2.17

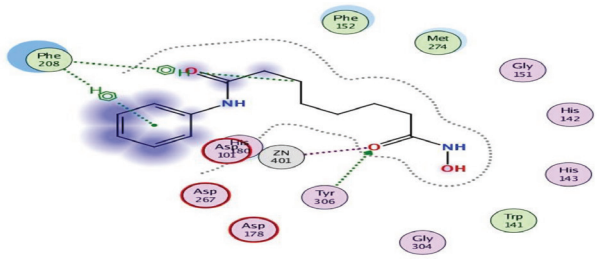

Fig. 3 **Demonstration of SAHA (Vorinostat) within the binding site of HDAC-8 and the mode of interactions.**

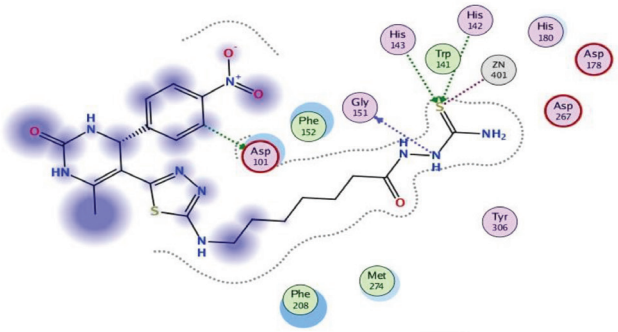

Fig. 4 **Demonstration of V c,t within the binding site of HDAC-8 and the mode of interactions.**

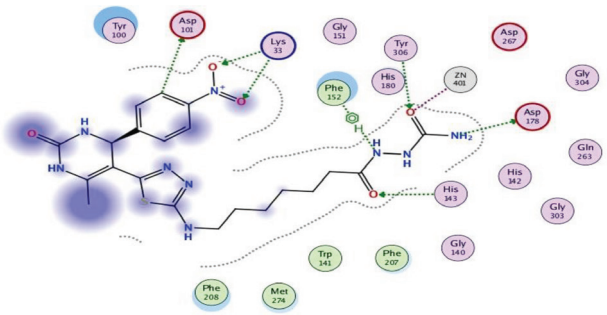

Fig. 5 **Demonstration of V c,s within the binding site of HDAC-8 and the mode of interactions.**

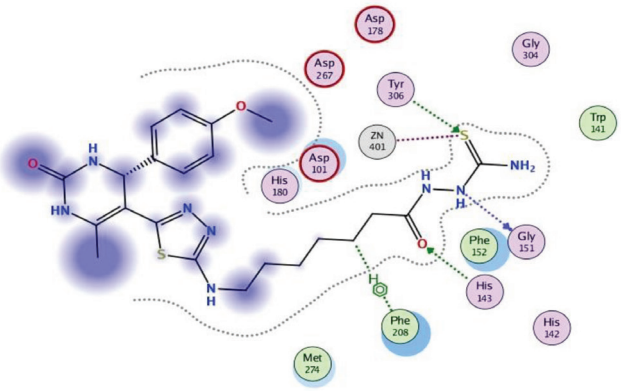

Fig. 6 **Demonstration of V d,t within the binding site of HDAC-8 and the mode of interactions.**

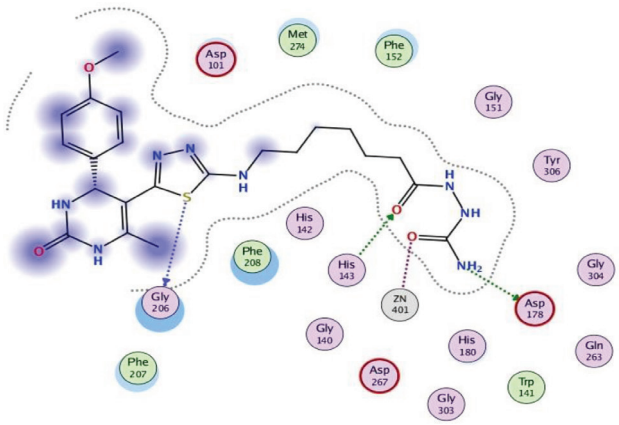

Fig. 7 **Demonstration of V d,s within the binding site of HDAC-8 and the mode of interactions.**

Synthesis of Compounds (I c,d – Vc,t, d,t)

Compound (I c,d) was synthesized by the reaction of aldehydes, Ethyl acetoacetate, urea and Ammonium chloride in

the presence of ethanol. The FTIR for both compounds were characterized by were characterized by disappearance of C=O band of aldehyde in the region around 1690 cm^{-1} the appearance of C=O amide bond at an area around 1743-1674 cm^{-1}, and the appearance of C=O ester bond at an area around 1701-1597 cm^{-1}. The ^{1}H-NMR for compounds (I c,d), ester analogs were characterized appearance of singlet signal due to the proton at the C of CH_3 near 2.3 ppm, and appearance of doublet signal due to the proton at C alpha to N of heterocyclic rings near 5.4 ppm and appearance of singlet signal due to the proton of NH heterocyclic rings near 9.9 ppm.

Compound (II c,d) was synthesized by the reaction of ester compounds (I c,d) and sodium hydroxide (15%) at 90°C. The FTIR for both compounds were characterized by the disappearance of C=O band of ester in the region around 1701-1697 cm^{-1}, and appearance of broad O-H band of carboxylic acid in the area around 3400-2500 cm^{-1}. The ^{1}H-NMR for compounds (II c,d), carboxylic acid analogs were characterized by the disappearance of triplet signal of proton of CH_3, quartet of CH_2 of ethyl ester near and the appearance of singlet signal of protons of OH near 12.3 ppm.

Compound (III c,d) was synthesized by the reaction of thiosemicarbazide with carboxylic acid compounds (II c,d) and 70% sulfuric acid in ethanol then neutralized with concentrated ammonia. The FTIR for both compounds were characterized by disappearance O-H band of carboxylic acid in the area around 3444-3200 cm^{-1} and C=O band of ester in the region around 1701-1697 cm^{-1}, and appearance of an NH a primary amine band at 3352-2966 cm^{-1}, C=N band in the region around 1600-1577 cm^{-1} and C-S-C band at 725-690 cm^{-1} The ^{1}H-NMR for compounds (III c,d), 1,3,4-thiadiazol-2-amino derivatives were characterized by the disappearance of the signal of proton OH near 12.3 ppm, and appearance of proton signal of NH_2 at the region near 7.02 ppm.

Compound (IV c,d) was synthesized by the reaction of compound (III c,d), ethyl-7- bromoheptanoate and dry K_2CO_3in anhydrous acetone The FTIR for both compounds were characterized by disappearance of an NH a primary amine band at 3352-3200 cm^{-1}, and appearance of C=O band of ester in the region around 1732 cm^{-1}, O-C band of ester at 1157-1203 cm^{-1}, C-H band of $(CH_2)_6$ at 1462-1427 cm^{-1} and C-H band of CH_2-CH_3 at 1377-1373 cm^{-1}. The ^{1}H-NMR for compounds (IV c,d), ester analogs characterized by the disappearance of proton signal of NH_2 at the region near 7.02 ppm, and apparent of NH proton as a signal at the region 7.4–7.5 ppm, several signal of CH_2 of the side chain, also apparent of triplet signal due to the proton at the C of CH_3 near 1.1 ppm.

Compound (V c,s, V d,s, Vc,t and V d,t) was synthesized by the reaction thiosemicarbazide or semicarbazide, KOH and compound (IV c,d) using saturated Ammonium chloride aqueous solution, ethyl acetate and Sodium sulfate. The FTIR for compounds (V c,s and V d,s) were characterized by disappearance of C=O band of ester in the region around 1732 cm^{-1} and the appearance of C=O amide band at 1604-1597 cm^{-1} , an NH a primary amine band at 3309-3032 cm^{-1}. The ^{1}H-NMR for compounds (V a,s and V b,s), were characterized by disappearance of proton signal of NH_2 at the region near 7.02 ppm, and apparent of NH proton as a signal at the region 7.4-7.5 ppm, several signal of CH_2 of the side chain, also apparent of triplet signal due to the proton at the C of CH3 near 1.1 ppm. The FTIR for compounds (V c,t and V d,t) were characterized by disappearance of C=O band of ester in the region around 1732 $cm^{-1}$and the appearance of C=O amide band at 1604-1597 cm^{-1}, an NH a primary amine band at 3309-3221 cm^{-1} , C=S band at 1261, 1253 cm^{-1}. The 1H-NMR for compounds (V a,t and V b,t), were characterized by disappearance of triplet signal due to the proton at the C of CH_3 near 1.1 ppm, and apparent of proton signal of NH_2 at the region near 6.4-7.2 ppm.

In Vitro Cytotoxicity Assay

The anticancer activity of compound (V c,s, V d,s, V c,t, and V d,t) were examined in the dose-response curve generated by Prism Pad 8.1 using nonlinear regression analysis for compounds in MCF-7 cells and HRT-18 cells is shown below figures. The IC_{50} values were obtained to a range of concentrations of compounds from (100–1.56 μM) by MTT assay. (Figures 8-10).

A) Cytotoxicity of compounds against human colon adenocarcinoma (HRT-18):

IC50 of V c,t in human colon adenocarcinoma (HRT-18) = 65.61 μM

B) Cytotoxicity of compounds against Breast cancer cell line (MCF7):

IC50 of V c,t in Breast Cancer Cell Line (MCF-7) = 0.65 μM
IC50 of V d,t in Breast Cancer Cell Line (MCF-7) = 0.71 μM

Discussion

According to the above-mentioned results, the synthetic compounds (V c,s and V d,s) does not show any cytotoxicity against the two cell line while (V a,t, V b,t,) are useful for the treatment of breast cancer and only (V c,t) useful for human colon adenocarcinoma, as they inhibit the HDAC enzyme through the presence of common pharmacophores consisting of three distinct domains as shown below:

(1) A surface recognition unit or cap group which usually a hydrophobic and aromatic group or may be heteroaromatic,[40] which interacts with the rim of the binding pocket. the cap group could be linked to the aliphatic linker group through either hydrogen-bond accepting or donating groups such as keto- and amide-groups.
(2) A zinc binding group (ZBG) or zinc binding domain (ZBD), such as the hydroxamic acid, benzamide, arboxylic acid, amide or biguanide groups,[41,42] hich coordinates with of Zn^{2+} ion in the active site outer surface.
(3) A linker domain that is either saturated or unsaturated with linear or cyclic structure, connects the cap group to the ZBD.[43] These are best illustrated by the classical, FDA-approved inhibitor suberoylanilide hydroxamic acid (SAHA).

Conclusion

In the recent decade, there have been several drugs to treat breast and colon cancer. However, there is still an unmet need to develop different types of drugs to reduce systemic toxicity and improve therapeutic efficacy. In the present study, we synthesized three compounds (V c,t, V d,t). The chemical structures of the synthesized compounds were confirmed by FT-IR

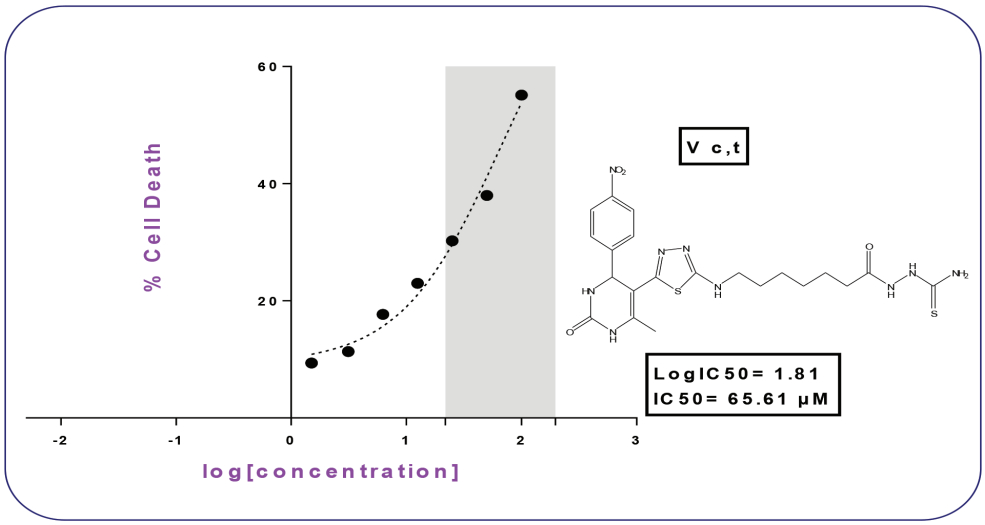

Fig. 8 **Dose-response curves of IC50 for V c,t. HRT-18 cells were treated for 72 hr. with 0.05, 0.15, 0.32, 0.75, 1.56, 3.12, 6.25, 12.5, 25, 50 and 100 µM dose ranges of V c,t. The dose response for V c,t was plotted over log transformed V a,t concentrations. IC50 values were determined using nonlinear regression analysis (Prism Pad 8.1). Results represent for triplicate data.**

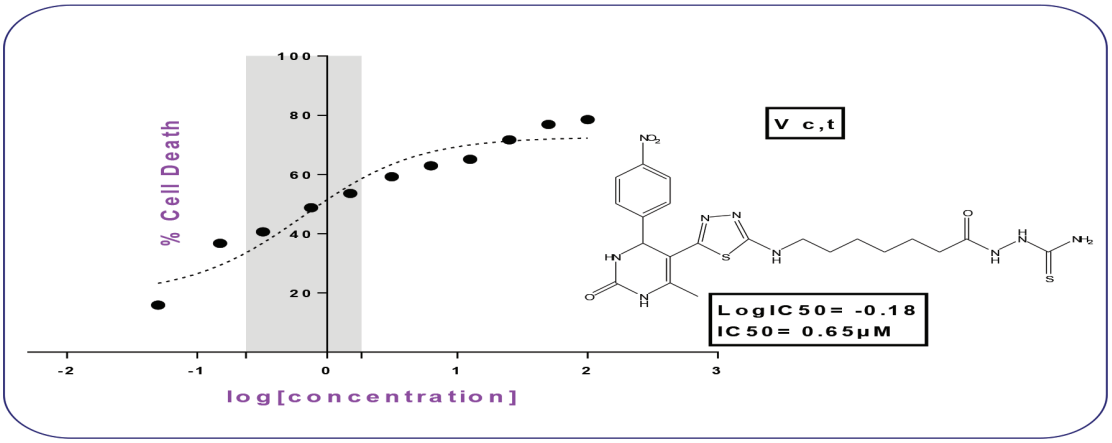

Fig. 9 **Dose-response curves of IC50 for V c,t. MCF-7 cells were treated for 72 hr. with 0.05, 0.15, 0.32, 0.75, 1.56, 3.12, 6.25, 12.5, 25, 50 and 100 µM dose ranges of V c,t. The dose response for V c,t was plotted over log transformed V a,t concentrations. IC50 values were determined using nonlinear regression analysis (Prism Pad 8.1). Results represent for triplicate data.**

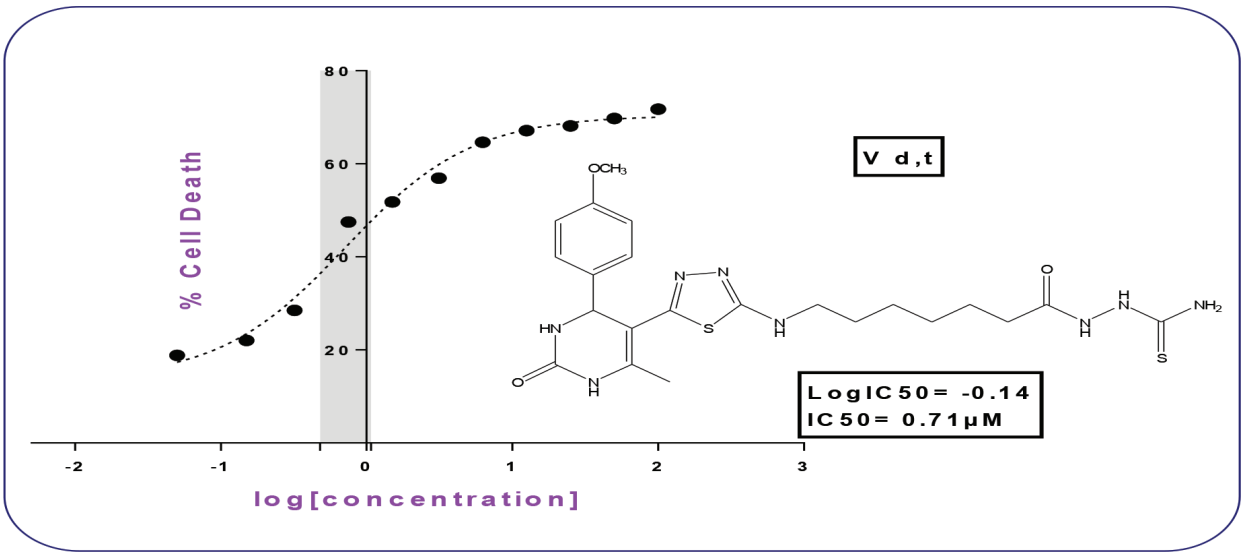

Fig. 10 **Dose-response curves of IC50 for V d,t. MCF-7 cells were treated for 72 hr. with 0.05, 0.15, 0.32, 0.75, 1.56, 3.12, 6.25, 12.5, 25, 50 and 100 µM dose ranges of V d,t. The dose response for V d,t was plotted over log transformed V d,t concentrations. IC50 values were determined using nonlinear regression analysis (Prism Pad 8.1). Results represent for triplicate data.**

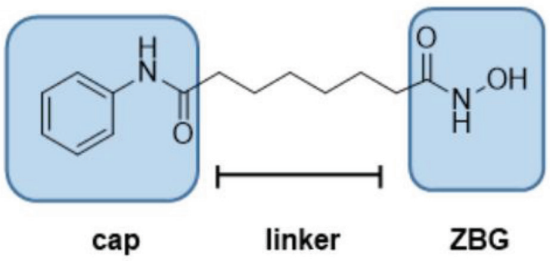

Fig. 11 **Structure of SAHA.**

and ^{1}H-NMR. MTT assay demonstrated In vitro cytotoxicity study against MCF-7 and HRT-18, for compounds (V c,t, and V d,t) show a good inhibition ratio to this cell line compared to SAHA. Therefore, these newly synthesized analogs may be represented as an exploitable source of new anticancer agents fighting breast cancer.

Acknowledgments

We thank the Department of Pharmaceutical Chemistry/College of the Pharmacy/University of Baghdad for their official support in this study.

Conflicts of Interest Disclosure

There are no conflicts of interest.

Competing Interests

The authors declare that they have no competing interests.

Source of Funding

Self-funded project.

References

1. Baretti M, Azad NS. The role of epigenetic therapies in colorectal cancer. Current Problems in Cancer. 2018;42(6):530 –47.
2. Baylin SB, Jones PA. Epigenetic determinants of cancer. Cold Spring Harbor perspectives in Biology. 2016;8(9):a019505.
3. Bunkar N, Pathak N, Lohiya NK, Mishra PK. Epigenetics: A key paradigm in reproductive health. Clinical and Experimental Reproductive Medicine. 2016;43(2):59.
4. Sharma S, Kelly TK, Jones PA. Epigenetics in cancer. Carcinogenesis. 2010;31(1):27 –36.
5. Manal M, Manish K, Sanal D, Selvaraj A, Devadasan V, Chandrasekar M. Novel HDAC8 inhibitors: A multi-computational approach. SAR and QSAR in Environmental Research. 2017;28(9):707 –33.
6. Parbin S, Kar S, Shilpi A, Sengupta D, Deb M, Rath SK, et al. Histone deacetylases: a saga of perturbed acetylation homeostasis in cancer. Journal of Histochemistry & Cytochemistry. 2014;62(1):11 –33.
7. Ruijter AJd, Gennip AHv, Caron HN, Kemp S, Kuilenburg ABv. Histone deacetylases (HDACs): characterization of the classical HDAC family. Biochemical Journal. 2003;370(3):737 –49.
8. Zhou H, Wang C, Ye J, Chen H, Tao R. Design, virtual screening, molecular docking and molecular dynamics studies of novel urushiol derivatives as potential HDAC2 selective inhibitors. Gene. 2017; 637:63 –71.
9. Eckschlager T, Plch J, Stiborova M, Hrabeta J. Histone deacetylase inhibitors as anticancer drugs. International Journal Of Molecular Sciences. 2017;18(7):1414.
10. Zwick V, Chatzivasileiou A-O, Deschamps N, Roussaki M, Simões-Pires CA, Nurisso A, et al. Aurones as histone deacetylase inhibitors: Identification of key features. Bioorganic & Medicinal Chemistry Letters. 2014;24(23):5497 –501.
11. Cappellacci L, Perinelli DR, Maggi F, Grifantini M, Petrelli R. Recent progress in histone deacetylase inhibitors as anticancer agents. Current Medicinal Chemistry. 2020;27(15):2449 –93.
12. Yoon S, Kang G, Eom GH. HDAC inhibitors: therapeutic potential in fibrosis-associated human diseases. International journal of molecular sciences. 2019;20(6):1329.
13. Yu C, He F, Qu Y, Zhang Q, Lv J, Zhang X, et al. Structure optimization and preliminary bioactivity evaluation of N-hydroxybenzamide-based HDAC inhibitors with Y-shaped cap. Bioorganic & Medicinal Chemistry. 2018;26(8):1859 –68.
14. Brindisi M, Senger J, Cavella C, Grillo A, Chemi G, Gemma S, et al. Novel spiroindoline HDAC inhibitors: Synthesis, molecular modelling and biological studies. European Journal of Medicinal Chemistry. 2018; 157:127 –38.
15. Liu R, Wang J, Tang W, Fang H. Design and synthesis of a new generation of substituted purine hydroxamate analogs as histone deacetylase inhibitors. Bioorganic & Medicinal Chemistry. 2016;24(7):1446 –54.
16. Manal M, Chandrasekar M, Priya JG, Nanjan M. Inhibitors of histone deacetylase as antitumor agents: A critical review. Bioorganic Chemistry. 2016; 67:18 –42.
17. Huang M, Zhang J, Yan C, Li X, Zhang J, Ling R. Small molecule HDAC inhibitors: Promising agents for breast cancer treatment. Bioorganic Chemistry. 2019; 91:103184.
18. Serban G, Stanasel O, Serban E, Bota S. 2-Amino-1, 3, 4-thiadiazole as a potential scaffold for promising antimicrobial agents. Drug Design, Development and Therapy. 2018; 12:1545.
19. Wu Q, Cai H, Yuan T, Li S, Gan X, Song B. Novel vanillin derivatives containing a 1, 3, 4-thiadiazole moiety as potential antibacterial agents. Bioorganic & Medicinal Chemistry Letters. 2020;30(10):127113.
20. Kasetti Ashok B, Singhvi I, Ravindra N, Shaik AB. Antimicrobial and antitubercular evaluation of some new 5-amino-1, 3, 4-thiadiazole-2-thiol derived Schiff bases. Rev Roum Chim. 2020;65(9):771 –6.
21. Mali JK, Sutar YB, Pahelkar AR, Verma PM, Telvekar VN. Novel fatty acid-thiadiazole derivatives as potential antimycobacterial agents. Chemical Biology & Drug Design. 2020;95(1):174 –81.
22. El-Hazek RM, El-Sabbagh WA, El-Hazek RM, El-Gazzar MG. Anti-inflammatory and analgesic effect of LD-RT and some novel thiadiazole derivatives through COX-2 inhibition. Archiv der Pharmazie. 2020;353(10):2000094.
23. Banik BK, Sahoo BM, Kumar B, Panda KC. Microwave Induced Green Chemistry Approach Towards the Synthesis of Heterocyclic Compounds via CN Bond Forming Reactions. Current Microwave Chemistry. 2021;8(3):204 –14.
24. Malygin A. Study on the antiepyleptic activity of the new amide derivative of valproic acid and 1, 3, 4-thiadiazole. Epilepsy and Paroxysmal Conditions. 2020;11(4):357 –63.
25. Zhang J, Wang X, Yang J, Guo L, Wang X, Song B, et al. Novel diosgenin derivatives containing 1, 3, 4-oxadiazole/thiadiazole moieties as potential antitumor agents: Design, synthesis and cytotoxic evaluation. European journal of medicinal chemistry. 2020; 186:111897.
26. Cascioferro S, Petri GL, Parrino B, Carbone D, Funel N, Bergonzini C, et al. Imidazo [2, 1-b][1, 3, 4] thiadiazoles with antiproliferative activity against primary and gemcitabine-resistant pancreatic cancer cells. European Journal of Medicinal Chemistry. 2020; 189:112088.
27. Perupogu N, Krishna CM, Ramachandran D. Design, synthesis and anticancer evaluation of 1, 2, 4-thiadiazole linked benzoxazole-quinazoline derivatives. Elsevier; 2020. p. 100482.
28. Azaam MM, Kenawy E-R, El-din ASB, Khamis AA, El-Magd MA. Antioxidant and anticancer activities of α-aminophosphonates containing thiadiazole moiety. Journal of Saudi Chemical Society. 2018;22(1):34 –41.
29. Cevik UA, Osmaniye D, Levent S, Sağlik BN, Çavuşoğlu BK, Karaduman AB, et al. Synthesis and biological evaluation of novel 1, 3, 4-thiadiazole derivatives as possible anticancer agents. Acta Pharmaceutica. 2020;70(4):499 –513.
30. Chidella K, Seelam N, Cherukumalli PKR, Reddy J, Sridhar G. Design and synthesis of novel 1, 2, 4-Thiadiazole linked imidazo [1, 2-b] pyridazine as anticancer agents. Chemical Data Collections. 2020; 30:100554.
31. Ding J, Liu J, Zhang Z, Guo J, Cheng M, Wan Y, et al. Design, synthesis and biological evaluation of coumarin-based N-hydroxycinnamamide derivatives as novel histone deacetylase inhibitors with anticancer activities. Bioorganic Chemistry. 2020; 101:104023.
32. Berman HM, Westbrook J, Feng Z, Gilliland G, Bhat TN, Weissig H, et al. The protein data bank. Nucleic Acids Research. 2000;28(1):235 –42.

33. Saloutin V, Burgart YV, Kuzueva O, Kappe C, Chupakhin O. Biginelli condensations of fluorinated 3-oxo esters and 1, 3-diketones. Journal of Fluorine Chemistry. 2000;103(1):17 –23.
34. K Hameed K, HS Hussain F. Ultrasound-Assisted Synthesis of Some New N-(Substituted Carboxylic Acid-2-yl)-6-Methyl-4-Substituted Phenyl-3, 4-Dihydropyrimidine-2 (1H)-One Carboxamides. Eurasian Journal of Science and Engineering. 2018;4(2).
35. Barbosa G, de Aguiar A. Synthesis of 1, 3, 4-Thiadiazole Derivatives and Microbiological Activities: A Review. Revista Virtual de Química. 2019;11(3):806 –48.
36. González-Martínez D, Fernández-Sáez N, Cativiela C, Campos JM, Gotor-Fernández V. Development of Biotransamination Reactions towards the 3, 4-Dihydro-2 H-1, 5-benzoxathiepin-3-amine Enantiomers. Catalysts. 2018;8(10):470.
37. Yang F, Zhao N, Song J, Zhu K, Jiang C-s, Shan P, et al. Design, synthesis and biological evaluation of novel coumarin-based hydroxamate derivatives as histone deacetylase (hdac) inhibitors with antitumor activities. Molecules. 2019;24(14):2569.
38. Deyrieux AF, Wilson VG. In vitro culture conditions to study keratinocyte differentiation using the HaCaT cell line. Cytotechnology. 2007;54(2):77–83.
39. Riss TL, Moravec RA, Niles AL, Duellman S, Benink HA, Worzella TJ, et al. Cell Viability Assays. Assay Guid Man [Internet]. 2016;1–25. Available from: http://www.ncbi.nlm.nih.gov/pubmed/23805433.
40. Sarah S. Jabbar, Mohammed H.Mohammed. Coumarin based-histone deacetylase HADC inhibitors. Egyptian Journal of Chemistry. 2022;65(7)379–384.
41. Duraid Al-Amily, Mohammed H. Mohammed. Design, Synthesis and Cytotoxicity Study of Primary Amides as Histone Deacetylase Inhibitors. Iraqi J Pharm Sci. 2019.Vol.28(2) .
42. Othman M. Sagheer, Mohammed H. Mohammed, Jaafar S. Wadi, and Zaid O. Ibraheem. Studying the Cytotoxic Activity of Newly Designed and Synthesized HDAC 2100346.
43. Miller TA, Witter DJ, Belvedere S. Histone deacetylase inhibitors. Journal of Medicinal Chemistry. 2003;46(24):5097 –116.